

MAGNETIC MICROACTUATION OF TORSIONAL POLYSILICON STRUCTURES

Jack W. Judy and Richard S. Muller

Berkeley Sensor & Actuator Center (BSAC) - An Industry/University/NSF Cooperative Research Center
Department of EECS, University of California, Berkeley, California 94720-1770 (U.S.A)

SUMMARY

A microactuator technology utilizing magnetic thin films and polysilicon flexures is applied to torsional microstructures. These structures are constructed in a batch-fabrication process that combines electroplating with conventional IC-lithography, materials, and equipment. A microactuated mirror made from a $430 \times 130 \times 15 \mu\text{m}^3$ nickel-iron plate attached to a pair of $400 \times 2.2 \times 2.2 \mu\text{m}^3$ polysilicon torsional beams has been rotated more than 90° out of the plane of the wafer and actuated with a torque greater than $3.0 \text{ nN}\cdot\text{m}$. The torsional flexure structure constrains motion to rotation about a single axis which can be an advantage for a number of microphotonic applications (e.g., beam chopping, scanning, and steering).

INTRODUCTION

Magnetic microactuation has recently been demonstrated by several research groups [1-6]. In most cases, magnetic-microactuator fabrication is not accomplished in a continuous batch process, instead it often requires the addition of steps such as manual assembly [1-3]. Recently, we demonstrated a microactuation technology that combines magnetic thin films with surface-micromachined cantilevers in a batch-fabrication process [4-5]. A similar actuation technology has recently been applied to arrays of microactuators for flow-stream control on aircraft-wing surfaces [6]. We describe here an application of batch-fabricated magnetic microactuators, which are made in a relatively simple process, to microstructures supported by torsion bars (Figure 1) that can be useful for optical-beam chopping, scanning, and steering. The microactuators we report here were driven by a magnetic field generated by an off-chip source.

TECHNOLOGY

The polysilicon structures are fabricated using a process developed earlier at BSAC to produce polysilicon surface-parallel microresonant systems [7]. To fabricate the new magnetically actuated devices, process steps are added just prior to releasing the polysilicon microstructures. At this point in the process, deposition of magnetic materials does not contaminate the conventional microelectronic and micromechanical fabrication steps. Furthermore, the additional steps do not add significantly to the thermal budget of the process. The micromechanical flexures are constructed with phosphorus-doped LPCVD polysilicon. An electroplated nickel-iron alloy, deposited using the procedure described by Ahn, Kim, and Allen [2], serves as the

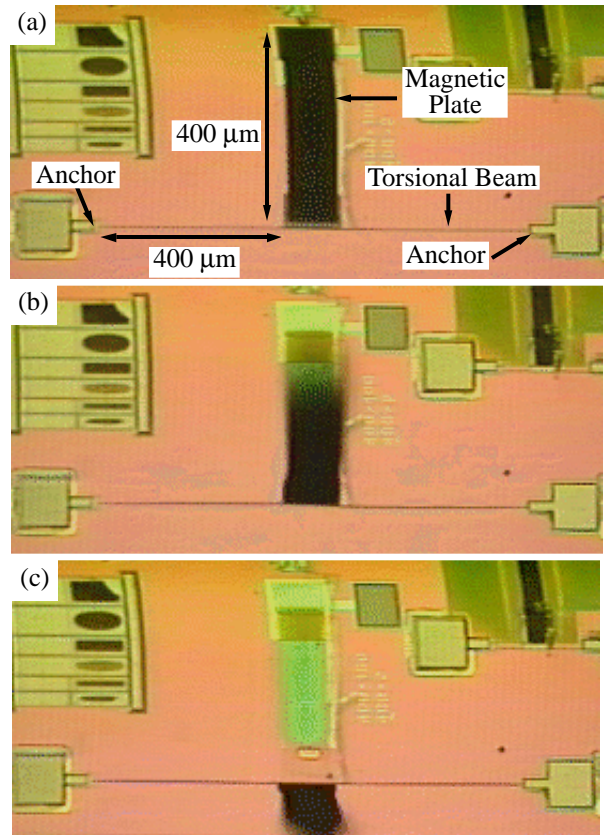


Figure 1. A torsion-bar-supported magnetic microactuator lifting out of the plane of the wafer.

magnetic material because of its relatively high saturation magnetization. The magnetic properties of NiFe have been well documented as a consequence of its widespread commercial use.

MECHANICAL ANALYSIS

The torsion-bar supported structure we built and studied is shown schematically in Figure 2. It consists of a narrow polysilicon beam, anchored to the substrate at both ends. At the center of the beam is a large plate of magnetic material attached on one side (Fig 2a). If a uniform magnetic field is applied to this structure, a pure moment without a translational force is induced. The pure moment or torque generated by the rigid magnetic plate rotates it through an angle ϕ (Fig. 2b). The torque can be translated to the axis of the torsional beams (Fig. 2c) to simplify the analysis.

Assuming each beam of length l is straight, has a uniform cross section, and is made of a homogeneous isotropic material that obeys Hooke's law, the torsional stiffness k_ϕ can be expressed as

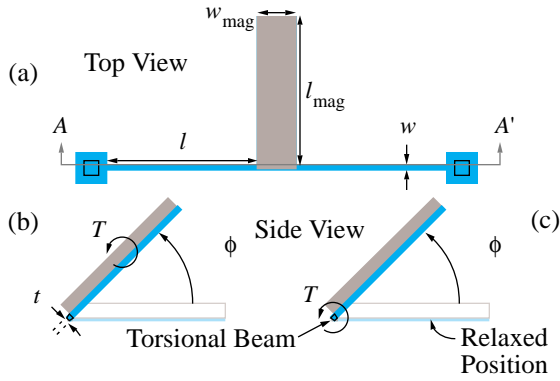


Figure 2. Schematic drawings of the mechanical structure.

$$k_\phi = 2 \left(\frac{KG + \sigma J}{l} \right) \quad (1)$$

where K is a cross-section dependent factor; the shear modulus is $G = E/(2(1-\nu))$ for elastic modulus E and Poisson's ratio ν ; the residual stress is σ ; and the polar moment of inertia is J [8]. For a beam with a rectangular cross section of width w and thickness t ,

$$K = \frac{a^3 b}{3} \left(1 - \frac{192 a}{\pi^5 b} \sum_{n=1,3,5,\dots}^{\infty} \frac{1}{n^5} \tanh\left(\frac{n \pi b}{2 a}\right) \right) \quad (2)$$

with $a = \min(w, t)$ and $b = \max(w, t)$ [9] and

$$J = \frac{1}{12} (w t^3 + w^3 t) \quad (3)$$

[8]. An important point to note is that k_ϕ is proportional to the smallest dimension of the beam cubed. Reducing the thickness of a beam with a $2 \times 2 \mu\text{m}^2$ cross section to less than $0.5 \mu\text{m}$, will reduce k_ϕ by a factor greater than 64. For our devices with $E = 170 \text{ GPa}$, $l = 400 \mu\text{m}$, $w = 2.2 \mu\text{m}$ and $t = 2.2 \mu\text{m}$; $G = 121 \text{ GPa}$, $K = 3.3 \times 10^{-24} \text{ m}^4$, $J = 3.9 \times 10^{-24} \text{ m}^4$, and $k_\phi = 2 \text{ nN-m/rad}$. The residual-stress dependent factor of Eq. (1) can be ignored because even for a stress as high as 1 GPa , the σJ term is only 1% of the KG term. The maximum shear stress τ_{max} in a torsion bar twisted by an angle ϕ is expressed by Timoshenko [9] as

$$\tau_{\text{max}} = \frac{1}{l} \left(2 G \phi a - \frac{16 G \phi a}{\pi^2} \sum_{n=1,3,5,\dots}^{\infty} \frac{1}{n^5} \tanh\left(\frac{n \pi b}{2 a}\right) \right) \quad (4)$$

MAGNETIC ANALYSIS

Although the behavior of permanent magnets in a magnetic field can be modeled using the concept of "effective magnetic charges" [4-6], soft magnetic materials, such as NiFe, are more accurately modeled using the concept of magnetic anisotropy and the demagnetizing field. When an external field \mathbf{H}_{ext} is applied at an angle α to the net magnetization vector \mathbf{M} of a sample (Fig. 3), the field exerts a torque of magnitude T_H on \mathbf{M} expressed as

$$T_H = |V_{\text{mag}} \mathbf{M} \times \mathbf{H}_{\text{ext}}| = V_{\text{mag}} M H_{\text{ext}} \sin \alpha \quad (5)$$

where V_{mag} is the magnet volume [10]. In a soft-magnetic material, T_H will rotate \mathbf{M} an angle θ away from its equilibrium direction, called the easy axis (Fig. 3). When \mathbf{M}

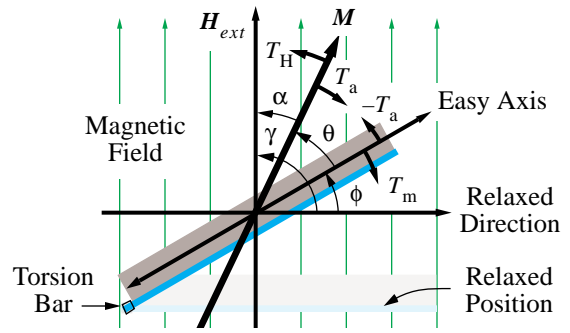


Figure 3. Schematic representation of the torques and angles involved in the material analysis.

rotates away from the easy axis, it increases the magnetic anisotropy energy W_a , given by

$$W_a = K_a \sin^2 \theta \quad (6)$$

where K_a is called the magnetic-anisotropy constant [10]. The magnetic-anisotropy constant can be subdivided into contributions due to shape, stress, crystalline, and induced anisotropies [5,10]. Because our low-stress magnetic films are polycrystalline and have no induced anisotropy, shape anisotropy is the essential determinant for K_a

$$K_a \approx K_{\text{shape}} = \frac{1}{2\mu_0} (N_c - N_a) M_s^2 \quad (7)$$

[10] where N_a and N_c are the length and thickness shape-anisotropy constants given by expressions derived by Osborn [11]; μ_0 is the permeivity of free space; and M_s is the saturation magnetization. As θ increases, the magnetic-anisotropy torque T_a , given by

$$T_a = -\frac{dW_a}{d\theta} = -K_a \sin 2\theta, \quad (8)$$

will increase in magnitude. Since the anisotropy torque attempts to bring \mathbf{M} and the easy axis back together, an equal but opposite torque $-T_a$ is exerted on the easy axis, and hence on the magnetic material itself (Fig. 3). If the magnetic material is attached to a flexure with angular spring constant k_ϕ , $-T_a$ will cause the magnetic material to rotate an angle ϕ from its original orientation. As ϕ increases, the mechanical restoring torque T_m , given by

$$T_m = -k_\phi \phi, \quad (9)$$

also increases. If the direction of the external magnetic field remains at a constant angle γ to the original direction of the easy axis, then although $\alpha = \gamma$ initially, it is reduced by θ and ϕ (Fig. 3), allowing Eq (5) to be rewritten as

$$T_H = V_{\text{mag}} M H_{\text{ext}} \sin(\gamma - \theta - \phi). \quad (10)$$

In a permanent-magnet analysis, the assumptions $M = M_s$ and $\theta = 0$ are made. However, it is often observed that the magnetization M of a soft-magnetic material varies as a function of H_{ext} and is less than M_s at low fields. As a sample is magnetized by an increasing field H_a , applied along \mathbf{M} and given by $H_a = H_{\text{ext}} \cos(\gamma - \theta - \phi)$, M increases and magnetic poles form on the ends of the sample. These

poles generate a field, called the demagnetizing field H_d , that opposes H_a . The magnitude of the demagnetizing field is $H_d = -N_M M / \mu_0$ where N_M is the shape-anisotropy coefficient of the sample in the direction of \mathbf{M} [10]. In our out-of-plane devices $N_M^2 = N_a^2 \cos^2 \theta + N_c^2 \sin^2 \theta$. The net field inside a magnetic sample H_i is the sum of the applied and the demagnetization fields $H_i = H_a + H_d$. Domain walls in a soft-magnetic material move to reduce H_i , resulting in $H_a \approx -H_d = N_M M / \mu_0$ from which we find

$$M \approx \mu_0 H_a / N_M. \quad (11)$$

Substituting H_a and N_M into (11) we solve for M

$$M \approx \min \left(\frac{\mu_0 H_{\text{ext}} \cos(\gamma - \theta - \phi)}{\sqrt{N_a^2 \cos^2 \theta + N_c^2 \sin^2 \theta}}, M_s \right). \quad (12)$$

In equilibrium, the field torque T_H , which rotates M away from the easy axis, is balanced by the anisotropy torque T_a , which acts to align M with the easy axis (Fig. 3). In turn, the torque on the sample $-T_a$ is balanced by the mechanical restoring torque T_m (Fig. 3). The resulting equilibrium condition is $|T_H| = |T_a| = |T_m| = T$. Using this equilibrium condition, ϕ , θ , and T can be solved by equating Eqns. (8), (9) and (10), and using M determined by Eq. (12). This set of transcendental equations can be solved numerically. A computer program was written to solve for ϕ , θ , M , and T . The calculations are compared with experimental values. For our devices with $l_{\text{mag}} = 430 \mu\text{m}$, $w_{\text{mag}} = 130 \mu\text{m}$, $t_{\text{mag}} = 15 \mu\text{m}$, and $M_s = 1.0 \text{ T}$ (as determined by film composition); $V_{\text{mag}} = 8 \times 10^{-13} \text{ m}^3$, $N_a = 0.0165$, $N_b = 0.0971$, $N_c = 0.8864$, and $K_a = 3.5 \times 10^5 \text{ J/m}^3$ (from Eq. (7)).

FABRICATION

After all the steps used to form the polysilicon structures are completed [7], an adhesion layer (10 nm Cr) and an electroplating-seed layer (100 nm Cu) are deposited by evaporation onto the polysilicon structure (Fig. 4a). At this point in the fabrication process, the photoresist plating mask is formed. Our earliest devices [4-5] were constructed using the ‘‘frame-plating’’ technique of Liao [12], to insure a uniform thickness, deposition rate, and electrodeposit composition. However, since the frame-plating process requires two thick-film photolithography steps, we have simplified the overall process by using a single thin-mask plating process. In this process the plating mask is formed by patterning a 2 μm -thick layer of photoresist to uncover the regions onto which the magnetic material will be electrodeposited (Fig. 4b). The plating solution was the same as that described in reference [2].

In our simplified process, the magnetic material is electroplated to a thickness many times that of the photoresist plating mask, causing the electrodeposit to ‘‘mushroom’’ over its edges (Figs. 4c and 5). Although such sloping sidewalls are undesirable for many in-plane microactuators, they do not adversely affect the performance of our devices. After depositing the magnetic material, the photo-

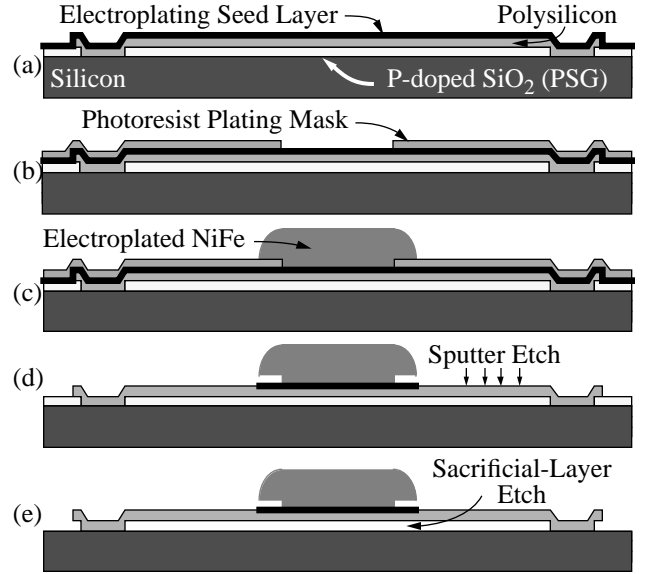


Figure 4. Fabrication process shown for the A-A' cross section (Fig. 2a).

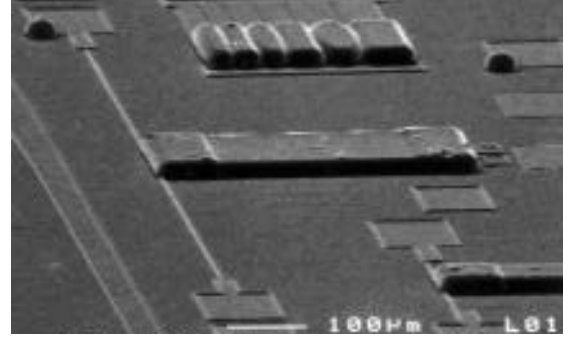


Figure 5. Scanning-electron microscope image.

resist is stripped and the Cu/Cr seed layer is removed by sputter-etching (Fig. 4d). The devices are then released in a concentrated two-minute HF (Fig. 4e).

EXPERIMENTAL RESULTS

Figure 1a shows optical photographs of a magnetic microactuator: (a) at rest without a magnetic field applied; (b) deflected approximately 45° by an applied magnetic field of ~5 kA/m; and (c) rotated into a vertical position with an applied magnetic field of ~10 kA/m. To measure the angular deflection of the devices as a function of the external magnetic field, the substrate was placed vertically between the poles of an electromagnet ($\gamma = 90^\circ$). As the magnetic field deflects the devices, the orientation of their edges is observed through a microscope. A radially marked graticule allows the angular deflections to be measured to an accuracy of $\pm 1^\circ$. A plot of the measured angular deflection ϕ as a function of H_{ext} is given in Fig. 6 for a device consisting of a $430 \times 130 \times 15 \mu\text{m}^3$ NiFe plate attached to a pair of $400 \times 2.2 \times 2.2 \mu\text{m}^3$ polysilicon torsional beams. Theoretical curves for ϕ as a function of H_{ext} are also plotted under the condition of constant magnetic saturation ($M =$

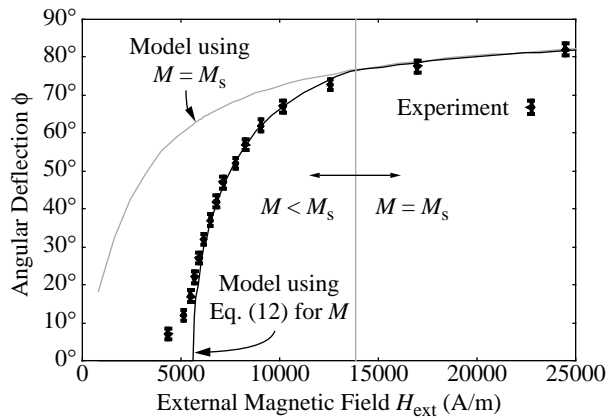


Figure 6. Comparison of theoretical calculations for angular deflection ϕ versus external field H_{ext} and experimental data.

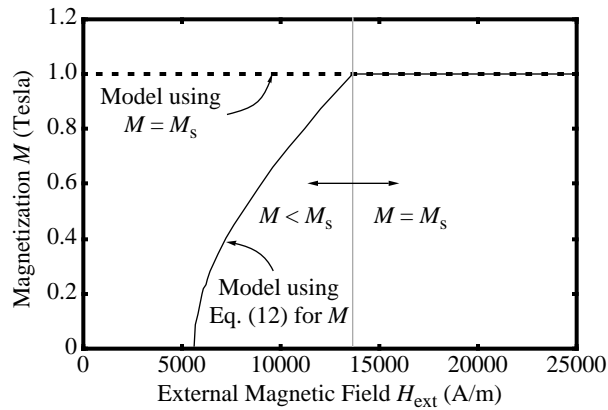


Figure 7. Magnetization of the soft-magnetic plate.

M_s) and also for the model described in this paper where M is given by Eq. (12). The theoretical predictions of the model presented in the previous section are in excellent agreement with the experimental results at low magnetic fields. The difference in results substantiates our assumption that the demagnetizing field reduces M as predicted by Eq. (12). A plot of M as a function of H_{ext} is given in Fig. 7, showing that $H_{\text{ext}} = 13.6$ kA/m saturates the deflected device.

The electroplated NiFe was measured to reflect 75% of the optical power of a laser beam, which was scanned over 135° with this actuated micromirror.

CONCLUSIONS

This research has demonstrated that magnetic films can be integrated with torsional-polysilicon flexures in a simplified batch-fabrication process. Prototype devices can be deflected 90° out of the plane of the wafer by a magnetic field of ~ 10 kA/m. The magnitude of the driving field required for a given angular deflection can be significantly reduced by thinning the torsional beams. The experimental behavior of these devices are well predicted by a magnetic model that includes magnetic anisotropy and the effects of the demagnetizing field. This actuation technology is well

sued for use in microphotonic applications, such as optical-beam chopping, scanning, and steering.

ACKNOWLEDGMENTS

The authors thank the staff of the Berkeley Microfabrication Laboratory for excellent support and service. We are grateful for helpful discussions with Dr. Hans H. Zappe and Prof. Jack H. Judy. The authors may be reached with j.judy@ieee.org, muller@eecs.berkeley.edu, and <http://www-bsac.eecs.berkeley.edu/~jjjudy> and ~muller. Funding for this research was provided by the National Science Foundation.

REFERENCES

- [1] B. Wagner, W. Benecke, G. Engelmann, and J. Simon, "Microactuators with moving magnets for linear, torsional, or multiaxial motion," *Sensors and Actuators A (Physical)*, Vol. A32, no. 1-3, pp. 598-603, 1992.
- [2] C. H. Ahn, Y. J. Kim, and M. G. Allen, "A planar variable reluctance magnetic micromotor with fully integrated stator and wrapped coils," *Proceedings of IEEE Micro Electro Mechanical Systems (MEMS '93)*, Fort Lauderdale, FL (February 7-10, 1993), pp. 1-6.
- [3] H. Guckel, T. R. Christenson, H. J. Skrobis, T. S. Jung, J. Klein, K. V. Hartojo, and I. Widjaja, "A first functional current excited planar rotational magnetic micromotor," *Proceedings of IEEE Micro Electro Mechanical Systems (MEMS '93)*, Fort Lauderdale, FL (February 7-10, 1993), pp. 7-11.
- [4] J. W. Judy, R. S. Muller, and H. H. Zappe, "Magnetic microactuation of polysilicon flexure structures," *Tech. Dig. Solid-State Sensor and Actuator Workshop (Hilton Head '94)*, Hilton Head Island, SC (June 13-16, 1994), pp. 43-48. (URL = <http://www-bsac.eecs.berkeley.edu/archive/conference/hh1994/jjudy/>)
- [5] J. W. Judy, "Magnetic microactuators with polysilicon flexures," *Masters Report*, Department of EECS, University of California, Berkeley, 1994. (URL = <http://www-bsac.eecs.berkeley.edu/archive/masters/jjudy/>)
- [6] C. Liu, T. Tsao, Y-C. Tai, J. Leu, C.-M. Ho, W.-L. Tang, and D. Miu, "Out-of-plane permalloy magnetic actuators for delta-wing control," *Proceedings of IEEE Micro Electro Mechanical Systems (MEMS '95)*, Amsterdam, the Netherlands, (January 29, February 2, 1995), pp. 7-12.
- [7] W. C. Tang, T.-C.H. Nguyen, M. W. Judy, and R. T. Howe, "Electrostatic-comb drive of lateral polysilicon resonators," *Sensors and Actuators A (Physical)*, vol. A21, no. 1-3, pp. 328-331, 1990.
- [8] R. J. Roark, *Roark's Formulas for Stress and Strain*, 6th Edition, Warren C. Young Editor, New York, McGraw-Hill Book Co., 1989.
- [9] S. P. Timoshenko and J. N. Goodier, *Theory of Elasticity*, 3rd Edition, New York, McGraw-Hill Book Co., 1970.
- [10] B. D. Cullity, *Introduction to Magnetic Materials*, Reading, Massachusetts, Addison-Wesley Pub. Co., 1972, p. 527.
- [11] J. A. Osborn, "Demagnetizing factors of the general ellipsoid," *Phys. Rev.*, vol. 67, no. 11 & 12, pp. 351-357, 1945.
- [12] S. Liao, "Electrodeposition of magnetic materials for thin-film heads," *IEEE Transactions on Magnetics*, vol. 26, no. 1, pp. 328-332, 1990.